

Wind tunnel boundary layer effects on the aerodynamic drag of model trucks

T. Lutz¹ and A.T. Sayers²

(Received November 1997; Final version December 1998)

The influence of the boundary layer on the floor of a wind tunnel on the aerodynamic drag of a model truck is examined. Through an extensive literature survey, a boundary layer suction system providing adequate ground simulation was designed and built. This suction drive was then tested to ensure that none of the main flow parameters of the airstream was influenced through its action. Testing on a model truck, featuring rotating wheels, with and without ground simulation, resulted in an increase in drag when the boundary layer was removed. It was also shown that the further a model protrudes into the original boundary layer, the less the drag.

Nomenclature

A_f	projected frontal area of model	m^2
C_D	drag coefficient $\{= D / (0.5\rho u_\infty^2 A_f)\}$	dimensionless
D	drag force	N
M	mass	kg
Q_f	actual volume flow rate	m^3/s
Q_t	theoretical volume flow rate	m^3/s
Re	Reynolds number $\{= u_\infty (A_f)^{1/2} / \nu\}$	dimensionless
t	time	s
u	velocity	m/s
u_∞	free stream velocity	m/s
x	distance along plate from leading edge	m
y	height above plate surface	m
z	transverse distance across plate surface	m
γ	yaw angle	degrees
δ	boundary layer thickness	m
ν	kinematic viscosity of air	m^2/s
ρ	density	kg/m^3

Introduction

One of the most important requirements of scale-model testing is that the results obtained therefrom reflect an accurate picture of the prototype's behaviour. It is therefore of fundamental importance that scale-model testing does not introduce any factors which could corrupt the test data. Classical wind-tunnel testing is characterised by a model resting on a balance, supported by a sting, and air is blown against the model. The model then experiences an array of forces and the wind tunnel balance measures these forces. This procedure however introduces a type of boundary layer, which is not experienced in the day-to-day operation of full-scale vehicles. When the air is blown across the wind-tunnel floor and walls, a boundary layer forms along these surfaces. The boundary layer arises due to the relative velocity between the air and the floor of the wind tunnel. It is most importantly characterised by a velocity profile within the boundary layer, increasing from zero on the tunnel floor to the free stream air velocity at some height above the floor at a distance further downstream. This effectively means that the mass flow in the boundary layer per unit height is less than in the adjacent free stream. Therefore, objects that protrude into this boundary layer will experience a different force than objects not protruding into this region, due to the lower mass flow rate. This paper examines the effect that the boundary layer has on the aerodynamic drag of a model truck through the removal of the boundary layer with the aid of suction.

All researchers in this field have stressed the importance of model detail and simulation and are in agreement that a very high degree of model detail is essential. Burgin *et al.*¹ felt that rotating wheels were essential, particularly when examining boundary layer effects. A minimum test Reynolds Number of 700000 is recommended,² whilst others,^{3,4,5} conducted tests at Reynolds Numbers ranging from 300000 to 4400000. However, Ohlson *et al.*³ concluded that this large range does not significantly affect the drag coefficient. The model height above the ground plane is also variable. Berndtsson *et al.*⁶ stated that if the boundary layer height was kept to 10% of the ground clearance, then its effect would be minimal. Garry⁷ suggested that the ground clearance be kept to 5% of the vehicle height, whilst Bearman *et al.*⁸ reasoned that the wheels should be kept in contact with the moving ground.

Rainbird *et al.*⁹ felt that a detailed survey of the test chamber with the ground simulation active was important. Garry⁷ achieved a reduction of 58% in the bound-

¹Former student

²Professor, Department of Mechanical Engineering, University of Cape Town, Rondebosch, 7700 South Africa

ary layer thickness and 90% in the boundary layer displacement thickness. Mercker *et al.*¹⁰ reduced the boundary layer thickness from 155 mm to 20 mm with a scoop and moving ground plane, whilst a reduction from 24 mm to 9 mm was achieved by Sardou¹¹ for the same arrangement. Similar results were achieved in the Porsche Wind Tunnel^{12,13} Sardou¹¹ found that aerodynamic drag increases with ground simulation; i.e. too low a drag is measured when there is no ground simulation during wind tunnel testing. Burgin *et al.*¹ showed that floor movement increases the drag by between 5% and 8%, whilst the research of Berndtsson *et al.*⁶ indicated that boundary layer suction yielded increased drag results of between 1.3% and 3.7% for a natural boundary layer height of 85 mm.

This paper describes aerodynamic drag force experiments carried out on a model truck where ground floor plane suction is used to remove the boundary layer. The effect on the boundary layer and subsequent aerodynamic drag on the vehicle are examined with and without rotation of the truck wheels, and with the inclusion of side skirts, and vehicle yaw to the incident wind.

Experimental apparatus

Wind tunnel

The experiments were carried out in a return circuit open jet wind tunnel test section driven by a 12 bladed variable pitch axial flow fan. The open jet test section was 870 mm × 580 mm, with corner fillets at the throat, and a working length of 1.6 m. The velocity variation across the empty test section was 1% and the turbulence intensity was 0.4%. The maximum velocity attainable in the test section was 36 m/s whilst the ratio between the area of the settling chamber and the area of the test section was 10:1. Pitot-static tube measurements taken in the empty test section along the horizontal axis of the jet showed a velocity variation of 2.6% over the 1.6 m jet length. This was small enough to be considered negligible. The overall dimensions of the model truck/trailer combination was 170 mm high by 100 mm wide by 880 mm long, resulting in a projected frontal cross-sectional area of 0.017 m². This gave a tunnel solid blockage ratio of 3.4% that was small enough to be considered negligible.¹⁴

Drag forces were measured electronically on a three component (lift/drag/yaw) strain gauge wind tunnel balance, the accuracy of the drag reading being to within 0.02 N.

Boundary layer suction system

The boundary layer suction apparatus consisted of a rectangular box, which featured a perforated top. At the sides of the box were the suction pipes, each 25.4 mm in diameter, which were connected to fans, which sucked the boundary layer air through the perforated top of the box. The top surface of this suction box was then the surface on which the model rested. This surface was completely

flat and reinforced with aluminium struts on the inside of the box. The surface was made up of five 1 mm thick galvanised steel sheets, each with the same length and width. Figures 1 and 2 show the hole pattern employed on this suction surface. Both patterns were characterised by the same centre to centre distance of the holes.

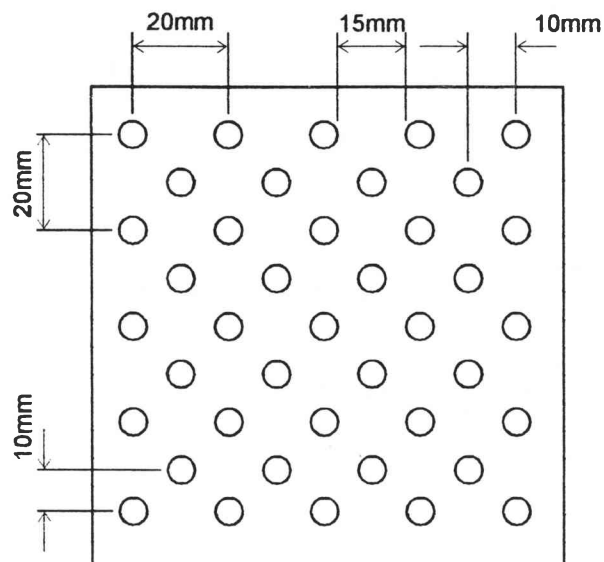


Figure 1 Arrangement of suction holes for basic suction with 5 mm diameter holes

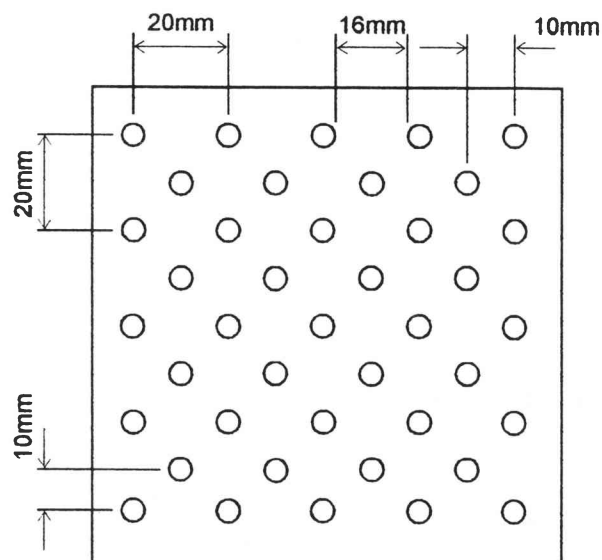


Figure 2 Arrangement of suction holes for distributed suction with 4 mm diameter holes

Two types of suction were used to remove the boundary layer. Over the first 100 mm of surface, basic suction was used which removed the boundary layer that had formed on the nose and forward sections of the perforated surface. This section of basic suction is shown in Figure 1. To remove the larger boundary layer that had already

formed, 5 mm diameter holes were drilled into this section. Also, the distance between each hole was 15 mm. The remainder of the surface used distributed suction, as shown in Figure 2, which meant that only the boundary layer that would build up over the 16 mm between the holes had to be removed. These holes were 4 mm in diameter.

Figure 3 shows the layout of the suction surface, with the 7 test locations, the outline of the model, and the suction pipes all clearly shown. The front of the box was fitted with a large boundary layer scoop, which removed the oncoming boundary layer already present on the wind tunnel floor. The sides of the suction floor were fitted with fences 40 mm high, to reduce the possibility of air being drawn onto the suction surface from the sides.

The entire suction box was mounted on a frame, which was in turn fitted with castors that could rotate and be locked in place. Along the top of the frame a three dimensional traverse allowed a pitot probe to be traversed along the length of the test section (x-direction), the width of the test section (z-direction), and the height of the test section (y-direction). This traversing probe was vital in surveying the test section air flow to ensure a high quality air stream, and was formed from a hypodermic needle, with the last 10 mm bent at 90° to the remainder of the needle and flattened. This resulted in a compact flat headed micro pitot probe suitable for measuring the stagnation pressure in the thin boundary layer. The reference free stream static pressure was measured with the static pressure tapping of a standard pitot-static probe located in the free stream. The pressure differential between the micro pitot tube and the free stream static pressure was used to calculate the flow velocity at any location within the boundary layer.

The model was a $\frac{1}{24}$ -scale model of the Ford Aero-master horse and US Reefer trailer unit and is shown in Figure 4. Overall length was 880 mm, width 100 mm, and height 170 mm. The model was suitably modified to allow for rotation of the wheels and the fitting of side skirts.



Figure 4 Model horse and trailer with skirts fitted

Suction box calibration

Previous investigations have revealed that many bluff bodies are not sensitive to over-suction. However, no detailed description of these bluff bodies was given and it was felt that the vertical velocity imposed on the body by the suction might influence readings, especially the lift force experienced by the body. In order that only the minimum amount of suction required to remove the boundary layer was applied, the suction box flow rate was calibrated against tunnel wind speed. With two fans connected to

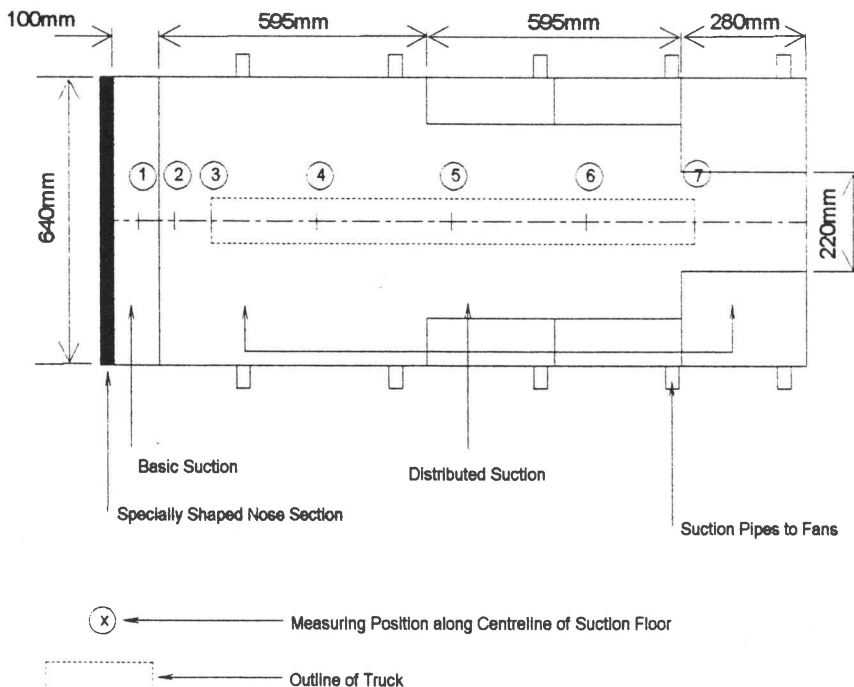


Figure 3
Layout of the
suction surface

the suction box, calibration was done by moving the micro pitot tube to point 3 (Figure 3), 4 mm in front of a suction hole and touching the floor. The air speed was set to the required value and the pressure difference (velocity head) between the micro pitot tube and the free stream static pressure was recorded for maximum suction. The flow rate through fan 2 was then slowly decreased until the velocity head began to drop. This indicated that as the flow rate of fan 2 was reduced, a threshold flow rate was reached where insufficient boundary layer air was being sucked away. This resulted in an excess of boundary layer airflow remaining close to the ground, and consequently the speed of the airflow in the still existing boundary layer was too high. The total discharge for both fans when this threshold flow rate was reached was determined for a range of tunnel wind speeds. The fan discharges were determined from pitot-static tube measurements taken across the discharge flange of each fan. Summing the discharge flow from both fans (Q_f), when the threshold value for fan 2 was reached, resulted in the total threshold suction flow rate for each wind speed setting in the tunnel for boundary layer removal. A theoretical approach was also used to verify the experimental results. Referring to Figure 1, it was reasoned that the boundary layer could grow for 15 mm for the basic suction, and in Figure 2, 16 mm for the distributed suction, until it was sucked off again by a successive hole. Using equation (1) for the growth of a laminar boundary layer,¹⁵ (Reynolds number below 500000) the mass flow in the boundary layer is given by

$$\frac{dM_{BL}}{dt} = \int_0^{\delta} \rho u dy \quad (1)$$

In a laminar boundary layer, the velocity distribution may be assumed to be given by

$$\frac{u}{u_{\infty}} = 1.5 \frac{y}{\delta} - 0.5 \left(\frac{y}{\delta} \right)^3 \quad (2)$$

Inserting equation (2) into equation (1) and dividing by the density of air gives the theoretical volume flow rate (Q_t) in the boundary layer over a unit width of 1 m, or

$$Q_t = \frac{5}{8} u_{\infty} \delta_x \quad (3)$$

The theoretical boundary layer thickness (δ_x) in the laminar flow region at any position x along a smooth flat plate is given by

$$\frac{\delta_x}{x} = 5 \left(\frac{u_{\infty} x}{\nu} \right)^{-\frac{1}{2}} \quad (4)$$

Referring to Figure 5, each 100 mm by 100 mm section of plate contains fifty suction holes. Assuming that each hole has to remove the boundary layer forming on the area directly in front of it, the required suction rate can be calculated. For the basic suction, using 5 mm holes, the distance between each hole is 15 mm and for the distributed suction using 4 mm holes, the distance is 16 mm. Each of these 100 mm by 100 mm sections has 50 such patches, as

shown by the cross-hatched lines. Thus equation (3) can be modified to first calculate the volume flow rate in the boundary layer for each patch and then summing the 50 patches per section will give the total boundary layer air that has to be sucked off over the 100 mm by 100 mm section. The distributed suction area features 64 100 mm by 100 mm sections and the basic suction area has six similar sections. The above is used to determine the theoretical volume flow rate that has to be removed from the entire test section. The subscripts denote that one hole has to suck off the boundary layer forming over 15 mm and the other hole has to suck off the boundary layer forming over 16 mm. The total theoretical volume of air (Q_t) that has to be removed is then calculated.¹⁶

$$Q_t = u_{\infty} (1.875\delta_{15} + 20.08\delta_{16}) \quad (5)$$

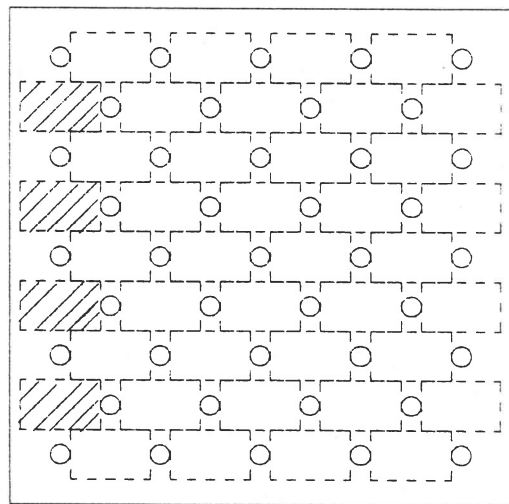


Figure 5 100 mm × 100 mm suction section with suction holes and patches (first four cross hatched for clarity) where the boundary layer is removed by the hole behind it

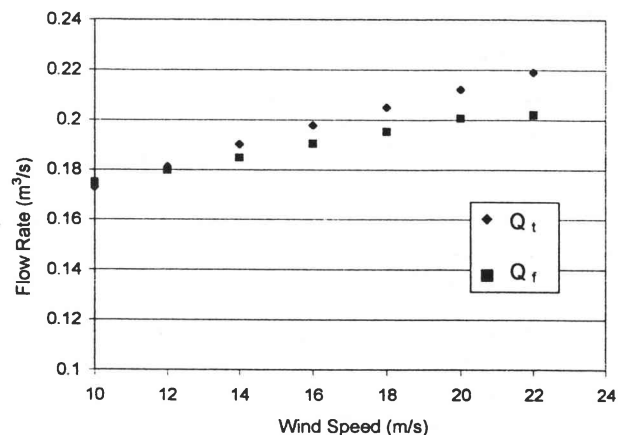


Figure 6 Actual and theoretical boundary layer flow rates

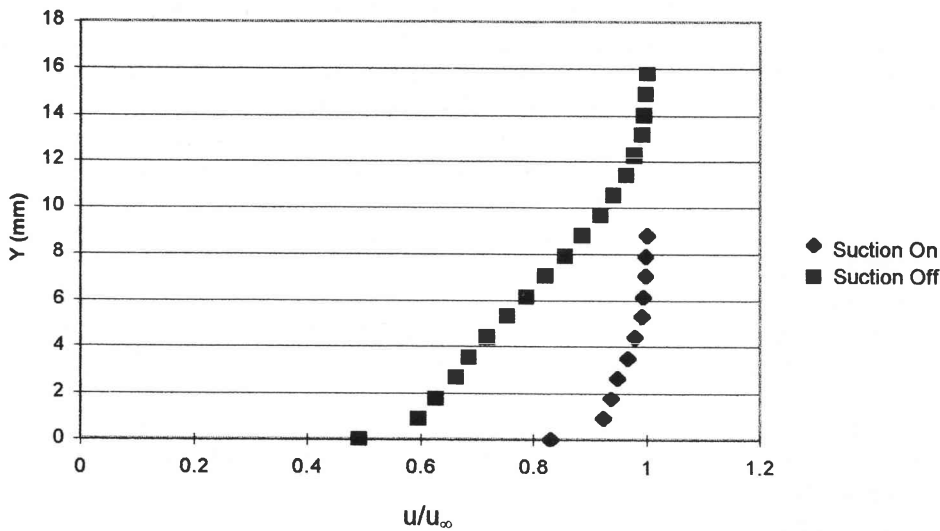


Figure 7
Velocity profiles
at station 3 with
suction on and off

Both δ_{15} and δ_{16} depend on the free stream speed over the test section. Figure 6 compares the theoretical (Q_t) and actual (Q_f) boundary layer flow rates. The results correlate well and show only a slight divergence at tunnel wind speeds over 18 m/s. This is caused by the fact that the available suction cannot remove enough of the boundary layer flow at higher wind tunnel speeds. Figure 7 compares the velocity profiles at station 3 with the boundary layer intact, i.e. with suction off, and with the boundary layer removed, i.e. with suction on. Station 3 corresponds to the position of the front of the model on the suction plate during subsequent drag tests.

Experimental method

The drag on the model was measured at various combinations of boundary layer criteria, wheel rotation, Reynolds number and yaw angle. Except where the Reynolds number was varied, it was kept constant at 20000 corresponding to a tunnel wind velocity of 22 m/s. Wheel rotational speeds were set to produce the required ground speed tangential velocity.

The boundary layer/wheel rotation combinations are classified as Types 1 through 4.

Type	Fan Suction	Wheel rotation
1	Off	On
2	Off	Off
3	On	On
4	On	Off

Wheel rotation signifies if the wheels were rotating or stationary, while fan suction indicates removal of the boundary layer. Suction 'On' means that the fans are switched on, the correct flow rate was selected and the boundary layer was removed. Rotation 'On' means that the wheels were rotating. The model was mounted in the

test section, as per Figure 4, on a 25 mm hollow support sting which protruded through the perforated ground plane and which was attached to a three-component lift/drag/yaw balance below the model. The cables for providing power to the wheel drive motors passed up through the inside of the sting. Before testing commenced, the aerodynamic drag of the sting was measured at the height corresponding to the truck wheels being in contact with the ground, and at other heights up to a maximum corresponding to a wheel height of 25 mm. At the commencement of each test, the model was set at the required yaw angle defined in Figure 8. Ground clearance was measured at the front wheels, i.e. a ground clearance of 5 mm indicates that the front wheels were 5 mm off the ground. All data were referred to a body axis system. Skirting was added during the final tests to determine the influence of lowering the overall ground clearance of the model body. A full description of all tests is provided by Lutz.¹⁶

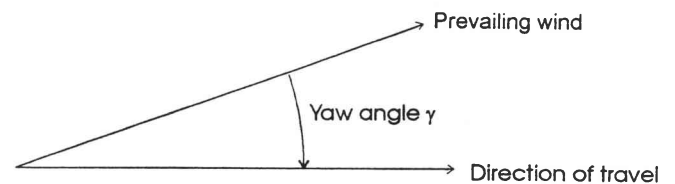


Figure 8 Yaw angle defined as that between the direction of motion and the prevailing wind

Results and discussion

In Figure 9, the basic type z simulation shows that as the ground clearance is increased, so the drag increases due to air striking the lower parts of the vehicle at a higher velocity and a higher mass flux. This trend of increasing

drag with ground clearance is also followed by the wheel rotation only (Type 1) simulation, but the effect of wheel rotation alone is to decrease the drag, particularly at small ground clearances. When boundary layer suction is provided, there is a general increase in drag for both the stationary wheel (Type 4) and rotating wheel (Type 3) simulations. The general effect of a drag reduction when the wheels are rotating is similar in trend to that obtained for sedan cars.¹⁷ It is also to be noted that the effect of wheel rotation decreases as the height of the model above the ground plane increase. Thus the model should be placed as close to the ground as possible, commensurate with the test requirements. Due to the softness of the rubber model tyres, deformation of the tyres occurred at the wheel rotation speed of 5500 r.p.m., and therefore the model was set at a height of 6 mm above the ground plane to preclude compromising the drag readings through tyre contact with the ground plane.

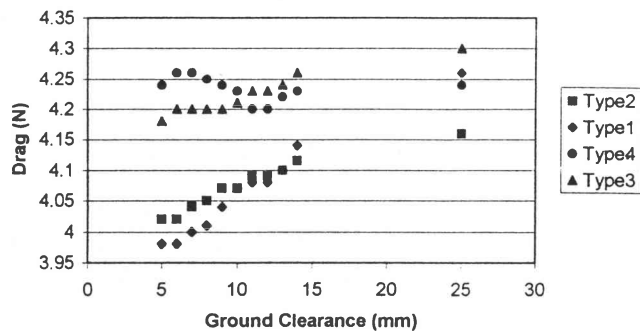


Figure 9 Drag force versus ground clearance for various simulations

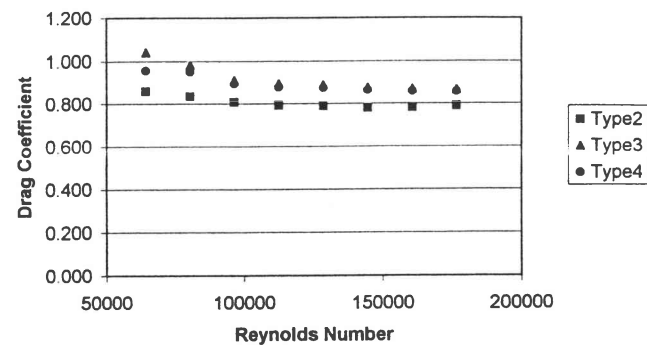


Figure 10 Drag coefficient versus Reynolds number with side skirts attached

Drag coefficient versus Reynolds number

A basic requirement for correct wind tunnel testing is that of dynamic similarity between the on-road and model test conditions, which is achieved through equality of Reynolds number for the two systems. However, this requirement

for the $\frac{1}{24}$ -scale model truck tested demands a wind tunnel speed of 24 times the road speed. At these speeds, compressibility effects would be introduced in the model flow regime. Tests at different Reynolds numbers with side skirting attached were carried out and the results are shown in Figure 10. Here, the drag coefficient remains fairly constant from a Reynolds Number of about 100000 and greater, based on the square root of the frontal area. Once again the boundary layer removal (suction on) increases the measured drag, but the effect of wheel rotation is negligible.

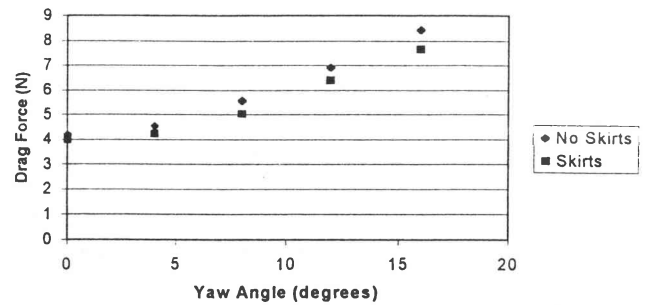


Figure 11 Drag force for type 3 simulation versus yaw angle

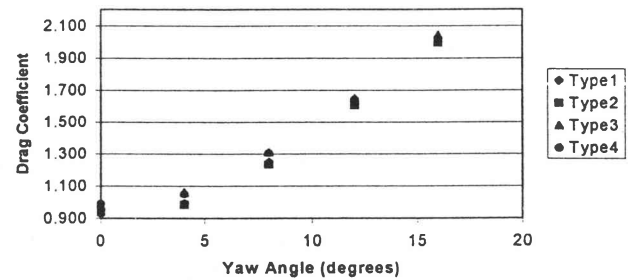


Figure 12 Drag coefficient for model without skirts versus yaw angle

Aerodynamic drag versus yaw angle

The graph presented in Figure 11 compares the model drag without skirts to that with skirts at the same non-rotating wheel clearance of 6 mm. The drag measured by the balance is the body axis component in the direction of motion of the truck resolved from the drag balance measurement. The skirts effectively lower the overall ground clearance between of the vehicle body 20 mm, leaving an 8 mm body to ground clearance. The model fitted with the skirts displays lower drag than the model without the skirts, due mainly to the smaller air flow on the underside of the model and its accompanying drag. This effect is amplified at higher yaw angles and is similar for all simulation types. Figure 12 shows the variation in drag coefficient with the skirts removed. In calculating the drag, both the drag force and

free stream velocity are resolved into the direction of motion of the truck. The simulation type hardly affects the drag for a given yaw angle. This is due to the increased pressure drag caused by the model being at an angle to the prevailing wind direction, when sharp edge separation from the front and rear edges of the model occurs. This increased pressure drag is much greater than any change in drag caused by the different types of simulation on their own. The rapidly increasing value of C_D with yaw is typical of an increasing wake.

Conclusions

This research has demonstrated the need for adequate ground simulation during vehicle model testing, especially if the test model is close to the ground plane. It is shown that a simple suction device could add sufficient energy to the overall flow by removing the retarded flow in the boundary layer. The suction device described in this paper removed 60% of the boundary layer thickness and 80 % of the boundary layer displacement thickness at the front of the model. The drag increases, which were measured for this model truck with the removal of the boundary layer, range from 3.8% to 10% with the skirts fitted. This is a large increase and can impact on the overall projected performance of the truck in day to day duty cycle operations.

References

1. Burgin K, Adey PC & Beatham JP. Wind tunnel test on road vehicle models using a moving belt simulation of ground effect. *Journal of Wind Engineering and Industrial Aerodynamics*, **22**, 1986, pp.227–236.
2. SAE Recommended Practice. Wind Tunnel Test Procedures for Trucks and Buses. *SAEJ12525*, 1968.
3. Ohlson ME & Schaub UW. Aerodynamics of Trucks in Wind tunnels: The Importance of Replicating Model Form and Detail, Cooling system and Test Conditions. *SAE 9203457*, 1992.
4. Saunders JW, Watkins S, Hoffmann PH & Buckley FT. Comparison of On-Road and Wind Tunnel Tests for Tractor-Trailer Aerodynamic Devices and Fuel Saving Predictions. *SAE850286*, 1985.
5. Kettinger JN. Tractor Trailer Fuel Savings with an Aerodynamic Device, A Comparison of Wind Tunnel and On Road Tests. *SAE820376*, 1982.
6. Berndtsson A, Eckert WT & Mercker E. The Effect of Ground Plane Boundary Layer Control on Automotive Testing in a Wind Tunnel. *SAE880248*, 1988.
7. Garry KP. Some Effects of Ground Clearance and Ground Plane Boundary Layer Thickness on the Mean Base Pressure of a Bluff Vehicle Type Body. *Journal of Wind Engineering and Industrial Aerodynamics*, **62**, 1996, pp.1–10.
8. Bearman PW, De Beer D, Hamidy E & Harvey JK. The Effect of a Moving Floor on Wind Tunnel Simulation of Road Vehicles. *SAE880245*, 1988.
9. Waudby-Smith & Rainbird WJ. Some Principles of Automotive Aerodynamic Testing in Wind Tunnels with Examples from Slotted Wall Test Section Facilities. *SAE850284*, 1985.
10. Mercker E & Knappe HW. Ground Simulation with Moving Belt and Tangential Blowing for Full Scale Automotive Testing in a Wind Tunnel. *SAE890367*, 1989.
11. Sardou M. Moving Ground and Reynolds number Effect on Tractor Trailer. *SAE870707*, 1987.
12. Vagt JD & Wolff B. Das Neue Meßzentrum für Aerodynamik, Zwei Neue Windkanäle bei Porsche, Teil 1. *ATZ*, 1987, pp.121–129.
13. Vagt JD & Wolff B. Das Neue Meßzentrum für Aerodynamik, Zwei Neue Windkanäle bei Porsche, Teil 2. *ATZ*, 1987, pp.183–189.
14. Sayers AT & Ball DR. Blockage Corrections for Rectangular Flat Plates Mounted in an Open Jet Wind Tunnel. *Proc. Instn. Mech. Engrs.*, **197c**, 1983, pp.259–263.
15. Holman JP. *Heat Transfer*, 7th edn. McGraw-Hill, 1992.
16. Lutz T. The Effect of the Boundary Layer Present in Wind Tunnels on the Aerodynamic Drag of a Model Truck. MSc Thesis. University of Cape Town, 1997.
17. Katz J. *Race Car Aerodynamics – Designing for Speed*. Robert Bentley Publishers, 1995.